

DOI: 10.1002/adma.200700418

Increasing the Complexity of Magnetic Core/Shell Structured Nanocomposites for Biological Applications**

By Verónica Salgueiriño-Maceira* and Miguel A. Correa-Duarte*



This Review article ponders core/shell structured nanoparticles that can be prepared with features that combine properties of different materials, including ligands that enhance their biocompatibility. These nanocomposites are not classified in terms of synthesis, but rather by how these features are distributed in the final morphology, attending to connected or isolated materials that end up in interacting or not-interacting functionalities. In particular, we have focused on magnetic core/shell-structured particles with a directly connected, coupled, or isolated second functionality. The current progress on methods in colloidal solution that have allowed the great development of these multifunctional magnetic and active spheres on biological and biomedical fields is reported.

1. Introduction

Shaping sub-micrometer-sized particles that exhibit more than two different properties, highly desirable for simultaneous and efficient technological applications, can be performed by assembling “building blocks” of several materials into nanocomposites, thereby providing bi-, tri-, or multifunctionality in contrast with their more limited single-component counterparts. In an ideal nanocomposite, the active nanoparticles (i.e., the carriers of the desired properties) would be far apart, because except for properties related to grain bound-

aries most of the physical properties of interest are those of non-interacting isolated nanoparticles. However, there are cases of interacting carriers that not only are suitable but also enrich the spectra of possibilities of these multifunctionalized nanocomposites. Remarkable is therefore the case of nanocomposites with a core/shell structure, which are promising candidates for integrating these multiple, interacting, or independent functionalities. This is accomplished by rearrangement of these nanometer-scale building blocks, giving place to superstructures that display various functions such as catalytic, magnetic, electronic, and optical properties and facilitate an understanding of the fundamental rules of their organization.

At the interface between materials science and biology such core/shell structures are emerging as a new challenge in the biotechnology field, very useful for enhancing or modifying the properties of the “building blocks” to exhibit a “biocompatible” behavior. Because of the rapidly increasing number of pharmaceutical applications and efforts in biomedical research, these particles have become the materials of choice.^[1,2] Indeed, the fact that nanoparticles are in the same size domain as many common biomolecules makes them appear to be natural companions in hybrid systems,^[3] leading to an explosive development of nanomedicine platforms in drug delivery and molecular imaging applications.^[2,4,5] Thus, nanomaterials have become increasingly important in the develop-

[*] Dr. V. Salgueiriño-Maceira
Departamento de Química-Física
Universidade de Santiago de Compostela
15782, Santiago de Compostela (Spain)
E-mail: vsalgue@usc.es
Dr. M. A. Correa-Duarte
Departamento de Química-Física
Universidade de Vigo
36310, Vigo (Spain)
E-mail: macorrea@uvigo.es

[**] V. S.-M. and M. A. C.-D. acknowledge the Isidro Parga Pondal Programme fellowships (Xunta de Galicia, Spain) and financial support from Xunta de Galicia, Spain (Project PGIDIT06PXIB314379PR).

ment of new molecular probes for in vivo imaging,^[6–9] both experimentally and clinically, used as unique building blocks in the design of supramolecular architectures. Therefore, supramolecular assemblies that take advantage of changes in several properties of the nanoparticles would be of particular value. Some types of nanoparticles have been already used clinically and in research protocols for the enhancement of magnetic resonance imaging (MRI) contrast, and include a multiple-mode imaging contrast combining magnetic resonance with biological targeting and optical detection. Therefore, nanoparticles have a typical tripartite constitution, featuring a core constituent material, a therapeutic and/or imaging payload, and biological surface modifiers which enhance the biodistribution of the nanoparticle dispersion.^[7] Among others, nanoparticulate imaging probes have included semiconductor quantum dots,^[10,11] magnetic^[12–14] and magnetofluorescent nanoparticles,^[15] gold nanoparticles, and nanoshells.^[16,17]

However, these may not be the only two areas where such systems will find interesting applications,^[18–20] because the high degree of control over particle morphology and an increased understanding of the displayed physical properties have led to the design of nanocomposites with specific applications, such as oncology imaging, solar cell technology, and light-emitting devices. As most applications rely heavily on the different materials that comprise the structures, the engineering of these nanocomposites, with or without isolated functionalities, is of paramount importance.

Herein, we have classified the assembly of building blocks into nanocomposites in terms of the way the different materials were brought together, thereby leading to interactions that sometimes result in properties different from those expected. The different building blocks reported have been connected via direct growth, junctions, or coupling chemistry, resulting in interacting and non-interacting characteristics that have allowed us to classify the nanocomposites in terms of their connected, coupled, or isolated functionalities.

2. Magnetic Functionality at the Nanometer Scale

The cases that are highlighted in this Review have started with an available magnetic material which was functionalized by insertion, attachment, or reduction on a second material helping to present a second functionality. There is therefore a fundamental motivation for the fabrication and study of nanometer-scale magnetic materials, driven by the dramatic change in magnetic properties that occurs when the critical length governing a phenomenon (e.g., magnetic, structural) is comparable to the nanoparticles or nanocrystal size.^[21–24] At this very small scale (on the order of tens of nanometers or less) magnetic particles exhibit remarkable phenomena such as superparamagnetism, where the magnetic moment of the particle as a whole is free to fluctuate in response to thermal energy, while the individual atomic moments maintain their ordered state relative to each other, leading to an anhysteretic,



Verónica Salgueiriño-Maceira received her Ph.D. degree in Chemistry from the Universidade de Vigo (Spain) in 2003. She has since worked as postdoctoral researcher at the Universität Duisburg-Essen (Germany) and at Arizona State University (USA) before joining the Universidade de Santiago de Compostela (Spain). Her current interests include metallic and magnetic nanoparticles, core/shell structured systems, and nanocomposites.



Miguel A. Correa-Duarte earned his Ph.D. degree in Chemistry from the Universidade de Vigo (Spain) in 2002, and since then has held postdoctoral positions at CAESAR (Bonn, Germany) and at Arizona State University (USA). He currently holds a researcher position at the Department of Physical Chemistry at the Universidade de Vigo. His interests include carbon nanotube functionalization, core/shell nanoparticles, and composites.

but still sigmoidal, magnetization versus magnetic field ($M-H$) curve), high field irreversibility, high saturation field, extra anisotropy contributions, or shifted loops after field cooling.

This is because of a fundamental change in the magnetic structure of ferro- and ferrimagnetic materials when sizes are reduced. The normal macroscopic domain structure transforms into a single-domain state at a critical size, which typically lies below 100 nm. These domains (groups of spins all pointing in the same direction and acting cooperatively) are separated by domain walls, which have a characteristic width and energy associated with their formation and existence. The motion of domain walls is a primary means of reversing magnetization. In large particles, energetic considerations favor the formation of these domain walls, but as the particle size decreases toward some critical particle diameter the formation of domain walls becomes energetically unfavorable and the particles are called single domain. Changes in magnetization can no longer occur through domain-wall motion and instead require the coherent rotation of spins, resulting in larger coercivities. As the particle size continues to decrease below the single-domain value, the spins are increasingly affected by thermal fluctuations and the system becomes superparamagnetic.^[25–27] Once this transformation occurs the mechanism of magnetization reversal can only be via the rotation of the magnetization vector from one magnetic easy axis to another via a magnetically hard direction, leading to a different class of magnetic materials of which the properties were first defined in 1948.^[28]

The underlying physics of superparamagnetism is founded on an activation law for the relaxation time τ of the net magnetization of the particle

$$\tau = \tau_0 \exp(\Delta E/k_B T) \quad (1)$$

where ΔE is the energy barrier to moment reversal, and $k_B T$ is the thermal energy. The energy barrier has several origins, including both intrinsic and extrinsic effects, such as the magnetocrystalline and shape anisotropies, respectively, but in the simplest case it has a uniaxial form and is given by $\Delta E = KV$, where K is the anisotropy energy density and V is the particle volume. This direct proportionality between ΔE and V is the reason that superparamagnetism (the thermally activated flipping of the net direction of the magnetic moment) is important for small particles, because for them ΔE is comparable to $k_B T$ at room temperature. However, it is important to recognize that observations of superparamagnetism are implicitly dependent not just on temperature, but also on the measurement time τ_m of the experimental technique used.

As a consequence of this rotation mechanism there exist magnetic nanoparticles that have a highly controllable coercivity, and this ability to control the coercivity has led to a number of significant technological advances in the fields of information storage and biomedical applications.^[12,13,29] Two of these biomedical applications are currently used. One involves a distortion in a magnetic field via MRI at a given site under examination, as the use of these magnetic nanoparticles

alters the contrast of certain types of cells, rendering them more visible. The second application lies in the production of controlled heating effects. Each cycle of a hysteresis loop of any magnetic material involves an energy loss proportional to the area of the loop. Hence, if magnetic nanoparticles having the required coercivity are positioned at a given site in the body, perhaps the site of a malignancy, the application of an alternating magnetic field can be used to selectively warm this site. This physical effect can therefore be used to either destroy cells directly or to induce a modest increase in temperature, so as to increase the efficacy of either chemotherapy or radiotherapy.

3. Magnetic Core/Shell Structured Particles Patterned with a Second Functionality

3.1. Directly Connected Functionalities

In the so called core/shell structured particles with directly connected functionalities, the shell is composed of an additional organic or inorganic material, uniformly and directly grown or attached around the magnetic core. Thereby, magnetic nanoparticles of different materials have been directly coated with organic, metallic, or semiconductor shells in order to impart a second functionality beside the magnetic one. Magnetic nanoparticles have found many practical and promising uses in biomedical fields that require enhanced biocompatibility and target specificity. Therefore, surface modification of these magnetic nanoparticles has become a key step to render them applicable in the biomedical field. In fact, having witnessed the explosive development of biomedical applications of bi-, tri-, or multifunctionalized nanocomposites, nanoscopic systems that incorporate therapeutic agents, molecular targeting, and diagnostic imaging capabilities are guiding the changes of their next generation. Nanocomposites that match these prerequisites have been designed by developing multifunctional polymeric micelles with cancer-targeting capability for controlled drug delivery and efficient MRI contrast characteristics.^[30] These novel micelles are composed of a chemotherapeutic agent (released through a pH-dependent mechanism), a specific ligand that can target tumor endothelial cells and subsequently induce receptor-mediated endocytosis for cell uptake, and a cluster of iron oxide nanoparticles loaded inside (for MRI detection). The structure to hold the three functionalities is a polymeric micelle built up from amphiphilic block copolymers of maleimide-terminated poly(ethylene glycol)-*block*-poly(D,L-lactide), and its structure is reflected in Figure 1. In this example, even in the case of directly connected functionalities being held in the same polymeric micelle, no interactions were reported.

Keeping in mind the magnetic building blocks related to the biomedical field, and maintaining the directly connected functionalities design, gold-coating has been chosen to render the surface of magnetic nanoparticles with unique chemical and optical properties. The synthesis of Fe oxide core/Au shell

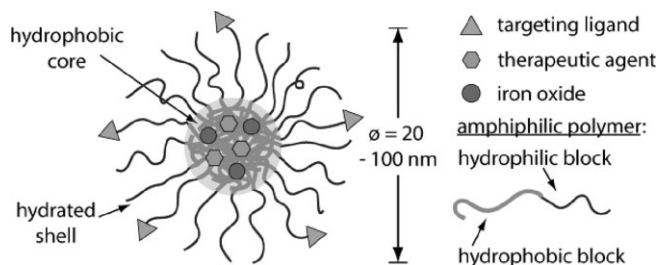


Figure 1. Schematic illustration of nanocomposites based on three key components: a chemotherapeutic agent that is released from polymeric micelles through a pH-dependent mechanism, a ligand that can target tumor endothelial cells, and a cluster of superparamagnetic iron oxide nanoparticles. Reproduced with permission from [30]. Copyright 2006 The American Chemical Society.

nanocomposites has attracted much interest owing to their possible biomedical applications, which may depend strongly on their stability in physiological solutions and on their chemically functionalized surface. This interest has therefore led to several examples which, depending on the chemical reactions, offer different cases of core/shell-structured nanoparticles.

The collective oscillations of free electrons of the Au shells cause an absorption peak to appear in the visible region, as in the case of pure gold nanoparticles.^[31,32] However, Halas and co-workers have postulated, based on the relative dimensions of the core radius and shell thickness of gold-coated silica spheres, that gold nanoshells (onto a dielectric silica core) show optical resonances that can be continuously tuned through wavelengths ranging from the ultraviolet to the infrared.^[33] The near-infrared (NIR) range becomes very useful in relation to the biomedical field because it improves the visualization of tissues owing to low scattering and absorption. This range spans a region where optical absorption in tissue is minimal because the tissue itself is mostly optically transparent, allowing imaging of deeper tissue structures.^[34] In the case of gold-coated magnetic nanoparticles, the different dielectric constants of the magnetic cores also contribute to a red-shift of the plasmon band from 520 nm, which would correspond to pure gold nanoparticles. However, this red-shift does not reach the NIR range, probably because the necessary core/shell ratio has not been accomplished yet. On the other hand, magnetic measurements of these core/shell particles have demonstrated that the outer gold shell has no influence on the core's magnetic behavior.

Au shells were formed by reduction of Au^{3+} onto Fe oxide surfaces by using a modification of Brown's iterative hydroxylamine seeding procedure,^[35] obtaining relatively big core/shell-structured nanoparticles with a shell thickness around 25 nm, but improving the polydispersity and sphericity of the particles after subsequent additions of the reduction agent.^[36] The core/shell formation was followed by UV-vis absorption spectroscopy, showing that as the ratio of Au to iron oxide increased, the surface plasmon peak blue-shifted toward the value expected for pure gold nanoparticles. Despite the possible influence of the different dielectric constant of the mag-

netic core on the electronic properties, Williams and co-workers argued that as the Au character increases the iron oxide becomes buried beneath the gold shell, thereby suppressing these possible dielectric effects.^[36] On a different approach to reduce gold onto iron oxide nanoparticles using hydroxylamine, core/shell particles with an average diameter of 70 nm were prepared.^[37] The UV-vis spectra showed a broad surface plasmon band, developed in the 500–800 nm range at the initial stage of the shell formation. As the number of iterations increased, the surface plasmon band blue-shifted toward 530 nm, although red-shifted compared to the previous case. This red-shift can be explained taking into account Halas calculations of optical resonances of gold nanoshells, which are a function of their core/shell ratio.^[38]

Gold-coated metallic iron and iron oxide nanoparticles have also been synthesized in reverse micelles of cetyltrimethylammonium bromide (CTAB), red-shifting the surface plasmon resonance from 528 to 555^[39] or to 560 nm,^[40] yet offering a core/shell ratio of ca. 2 in the second case. The different surface plasmon band position can be explained by taking into account the different core/shell ratios (not reported in the first case) or a different homogeneous degree of coating.

In the synthesis of these nanocomposites formed by more than one material, the arrangement of a large interface between the two materials is frequently observed when the lattice constants of the two components do not differ significantly or when the control of synthesis parameters allows the interfacial energy to be kept low. These prerequisites therefore lead to the formation of core/shell-type hybrid nanocomposites. The case of Au and Fe, however, is at least surprisingly bizarre. In fact, by thermolyzing gold and iron precursors almost simultaneously, a dumbbell-like structure was formed instead of a core/shell system.^[41] The dumbbell structure was formed through (nucleation) epitaxial growth of iron oxide on the Au seeds, and the growth could be affected by the polarity of the solvent, because the use of a more polar solvent led to flower-like composite particles (see Fig. 2).^[41] The dumbbell-like structured $\text{Au}/\text{Fe}_3\text{O}_4$ composite nanoparticles red-shift the surface plasmon band owing to its nanocontact with the magnetic

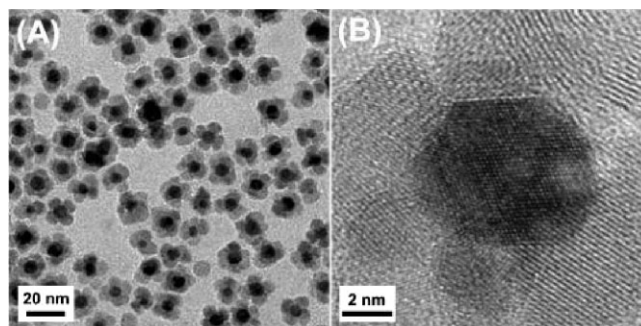


Figure 2. Transmission electron microscopy (TEM) and high-resolution TEM (HRTEM) images of flower-like $\text{Au}-\text{Fe}_3\text{O}_4$ nanoparticles. Reproduced with permission from [41]. Copyright 2005 The American Chemical Society.

component. Au particles with sizes ranging from 5 to 20 nm in diameter show a characteristic collective oscillation frequency of the plasmon resonance, giving rise to the plasmon resonance band at around 520 nm.^[31,32,42] The peak at 520 nm for Au nanoparticles is independent of the size and concentration of the particles, but the width was found to increase with decreased size of the Au particles. However, once attached to Fe₃O₄ the Au particles show the plasmon absorption at 538 nm, which means a red-shift of ca. 18 nm. Yu et al. pointed out a charge variation of the Au particles within the dumbbell structure because the red shift of the surface plasmon band can indicate an interface communication between Au and Fe₃O₄ that results in deficient electron population on Au.^[41]

Gold has also been used together with magnetic materials to pattern silica spheres with optical and magnetic functionalities, through a combination of colloidal methods and different techniques.^[43] The strategy developed by Correa-Duarte and co-workers was based on electron-beam evaporation (EBE), which allows the deposition of metallic thin films onto silica spheres. By means of this elaborated procedure, asymmetrically functionalized silica spheres were synthesized, meaning that different materials (gold and nickel) were deposited onto opposite hemispheres of the same particles. Both metals could be deposited onto silica spheres (average diameter 360 nm, synthesized following the Stöber method^[44]) by EBE in two consecutive steps. Metallic gold was first evaporated on one side, and once the upper hemisphere was coated polymerization of styrene was initiated on top of this monolayer. This thin polymeric film was then used to remove the half-coated monolayer of silica spheres from the substrate in such a manner that the monolayer remained trapped with the half-coated particles embedded in the polymeric film. The naked and polymer-free hemispheres were then exposed to the evaporation source again, using nickel for the second half-coating. Upon completion of this two-step evaporation process, bimetallic colloids with an asymmetric core/shell morphology were obtained, having the two functionalities directly connected along the equator of the silica spheres. Although this case would also fit in the group of silica-based nanocomposites (Section 3.3 of this Review), the fact of having both materials directly connected has led us to include them in this first classification. Figure 3a and b shows a schematic illustration

of these two-sided spheres (Janus-particle morphology)^[20,45,46] and a scanning electron microscopy (SEM) image, respectively, of a silica sphere with a half-shell of gold and half-shell of nickel, providing a unique construction that would have been extremely difficult to prepare using standard colloid synthesis.

3.1.1. The Luminescent Functionality

Luminescence has become one of the most appreciated functionalities in magnetic systems because both properties turn out to be more advantageous when combined, for example in bio-detection, biosensing, bioseparation, and targeted drug delivery applications. The fundamental motivations for the inclusion of photoactive molecules or semiconductor quantum dots (QDs) in nanocomposites fabrication protocols are the unique optical properties they display, which have become important tools widely used in biology. Luminescence is the emission of ultraviolet, visible, or infrared photons from electronically excited species. Luminescent species can be of very different kinds, including organic (e.g., aromatic hydrocarbons, fluorescein, rhodamines, aminoacids), inorganic (e.g., uranyl and lanthanide ions, doped glasses, crystals), and organometallic compounds (e.g., ruthenium complexes, complexes with lanthanide ions and with fluorogenic chelating agents).^[47] Fluorescent species are currently used as probes for the investigation of physicochemical, biochemical, and biological systems; however, the development of high-sensitivity and high-specificity probes that lack the intrinsic limitations of organic dyes and fluorescent molecules is of considerable interest in molecular and cellular biology for imaging and medical diagnostics. Conventional dye molecules have broad emission spectra with long tails at red wavelengths that introduce spectral cross talk between different detection channels, making quantization of the relative amounts of different probes difficult.^[48] In fact, ideal probes should emit at spectrally resolvable energies and have a narrow, symmetric emission spectrum, and the whole group of probes should be excitable at a single wavelength.^[49] In comparison with organic fluorophores, colloidal semiconductor QDs (single crystals a few nanometers in diameter whose size and shape can be precisely controlled by the duration, temperature, and ligand molecules used in the synthesis)^[50] have composition- and size-dependent absorption and fluorescence emission ranging from visible to infrared wavelength, large absorption coefficients across a wide spectral range, and very high levels of brightness and photostability.^[2] For nanocrystals smaller than the so-called Bohr exciton radius (a few nanometers), energy levels are quantized, with values directly related to the QDs size (an effect called quantum confinement, hence the name “quantum dots”). In the case of QDs the radiative recombination of an exciton leads to the emission of a photon in a narrower, symmetric energy band, compared to the red-tailed emission spectra of most fluorophores.^[5] Two of the primary applications of QDs are in optoelectronics^[51] and in fluorescence-tagging techniques. The development of these nano-

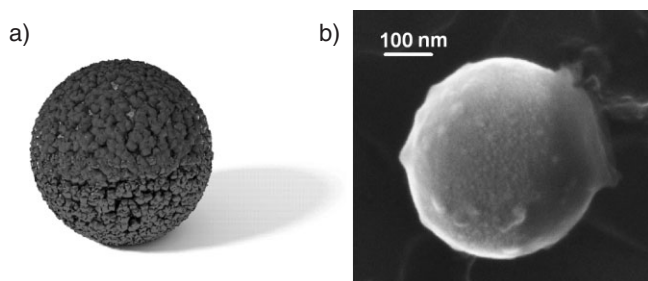


Figure 3. Illustration (a) and SEM image (b) of an asymmetrically coated silica sphere with opposite half-shells of gold and nickel. Reproduced with permission from reference [43]. Copyright 2005.

crystals for biological labeling has opened up new possibilities for many multicolor experiments and diagnostics, in direct immunolabeling, in situ hybridization, or in applications such as cytometry and immunocytochemistry. They have been already tested in DNA array technology, immunofluorescence assays,^[52] and cell and animal biology. They have been also used in immunofluorescence labeling of fixed cells and tissues, immunostaining of membrane proteins,^[53,54] and in fluorescence of in situ hybridization on chromosomes^[55] or combed DNA.^[56]

There are numerous strategies, that have been designed taking advantage of wet-chemistry methods, available for the synthesis of luminescent magnetic core/shell structured nanocomposites. CdSe-coated cobalt (Co@CdSe) nanoparticles are a recent option, prepared by controlled deposition of the semiconductor material onto the already synthesized Co nanocrystals,^[57] retaining the spherical shape of the seed core and exhibiting a uniform shell 2–3 nm thick. As a possible mechanism, Klimov and co-workers suggested the shell formation as a random nonepitaxial nucleation of CdSe onto the magnetic surface, followed by growth and nanocrystallite merging.^[57] This is a clear example of interacting functionalities, as shown in Figure 4, where the contrast between the Co and the CdSe shell is easily distinguishable in both transmission electron microscopy (TEM) and high-resolution (HR) TEM images. The fact of not having the functionalities isolated implies an interface between them, leading to a decrease in the blocking temperature (from 350 to 240 K) of the magnetic nanoparticles before and after being coated with CdSe, which was neither observed when magnetic-optical nanocrystals were obtained as dimers,^[58,59] nor when iron oxide nanoparticles were coated with gold.^[36,37,39,40] Furthermore, when comparing the magnetic properties of the Co nanocrystals, the same coercive field but a large drop in saturation magnetization per gram were determined in the core/shell structures owing to the presence of the nonmagnetic CdSe phase. Taking into account that the coercivity of the nanocrystals depends mainly on the magnetocrystalline anisotropy and the domain size of the particles, and the fact that the coercivity did not change after coating, it can be concluded that the coercivity is determined mainly by magnetocrystalline anisotropy rather than surface anisotropy, which would be sensitive to this surface modification.

The second consequence of having directly connected functionalities in these nanocomposites is the observation of a relatively large Stokes shift compared to monodisperse CdSe nanoparticles of similar size. This larger Stokes shift in the Co@CdSe nanoparticles may be related to the effect of a close-proximity nanomagnet or to the CdSe shape anisotropy, because pairs of neighboring domains are sufficiently well associated.^[60] Furthermore, Kim and co-workers^[57] claimed that the presence of the magnetic core significantly affected the effective strength of the “emitting” optical transition of the semiconductor shell, likely through modifying the spin structure of the lowest excitonic state.^[61]

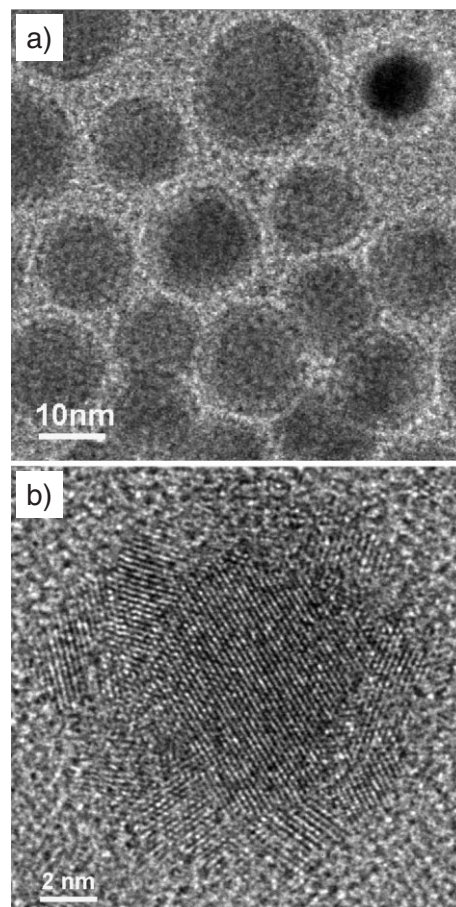


Figure 4. TEM (a) and HRTEM (b) images of CdSe-coated cobalt nanoparticles. Reproduced with permission from [57]. Copyright 2005 The American Chemical Society.

A similar method was exploited for preparing an analogous system of a semiconductor shell coating a magnetic core; in this case, CdS-coated FePt (FePt@CdS) nanoparticles.^[62] Amorphous CdS was deposited onto the surface of FePt nanoparticles to form a metastable core/shell structure, in which the CdS shell became crystalline upon heating. Because of the incompatibility of the lattices of FePt and CdS and the surface tension when dispersed in solution, the FePt@CdS core/shell nanoparticles evolved into heterodimers of CdS and FePt nanocrystals, as indicated in Figure 5.

Bifunctionalized core/shell structured nanoparticles that possess magnetic and up-conversion fluorescence properties were also synthesized by using iron oxide nanoparticles (5–15 nm average diameter) as the core to be covered with ytterbium and erbium co-doped sodium yttrium fluoride.^[63] Once coated with the up-converting fluorescent materials the nanoparticles reached an average diameter in the range of 53–87 nm, and green and red up-conversion emissions were observed with 980 nm infrared excitation. Lu and co-workers claimed that in this case no influence from the magnetism of the core was found.^[63] To be able to use these bifunctional

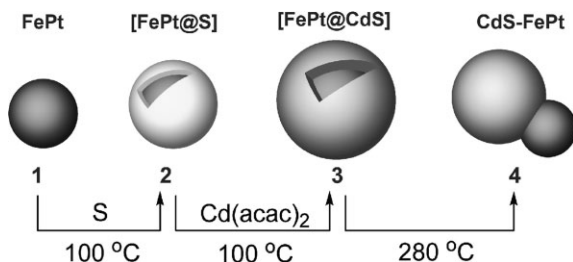


Figure 5. Schematic illustration for the synthesis of CdS/FePt dimers. FePt nanoparticles (1) are initially coated with suitable amounts of elemental sulphur, which in the subsequent step likely produces a metastable core/shell nanostructure, in which CdS is amorphous (2). Raising the solution temperature to 280 °C converts CdS from its amorphous to its crystalline state and results in heterodimers of CdS and FePt nanoparticles (4). acac: acetylacetonate. Reproduced with permission from [62]. Copyright 2004 The American Chemical Society.

nanoparticles in processes of bioseparation and biodetection they were further coated with silica and functionalized with 3-aminopropyltrimethoxy silane (APS), positioning amino groups on the surface of the nanoparticles.

By contrast, bifunctionalized particles were also prepared by simultaneously embedding fluorescent Cd/ZnS QDs and maghemite nanoparticles into hydrazinized styrene/acrylamide (H_2N -St-AAm) copolymer nanospheres.^[64] The St-AAm copolymer nanospheres were synthesized first from styrene and acrylamide by a modified method of emulsifier-free polymerization,^[65] offering nanospheres with a mesoporous surface, thus providing an entry route for nanoparticles. The strategy takes into account that the hydrophilic groups of the polymer are located towards the outer surface of the nanospheres, while the hydrophobic moieties are found at the interior, leading to the formation of hydrophobic hollow cavities, since the nanospheres are synthesized in an aqueous solution. This hydrophobic nature of the hollow cavity helps relocating both hydrophobic luminescent QDs and magnetic nanoparticles inside, dispersed in a weakly polar organic solvent. In this case, the magnetic nature of the iron oxide nanoparticles influences the fluorescence emission and can be tuned depending on the relative dosages of both kinds of nanoparticles. Analogously, Wang and co-workers covalently coupled hydrazide-containing bifunctional particles with IgG, avidin, and biotin to generate novel fluorescent-magnetic-biotargeting trifunctional nanospheres.^[66]

One more option for keeping together magnetic and luminescent functionalities was reported with the synthesis of a hybrid material comprising QDs and iron oxide nanoparticles encapsulated in a silica shell.^[67] The process followed makes use of a reverse microemulsion medium into which both types of nanobuilding blocks for the silica coating are introduced. As the silica coating reaction progressed, the absorption and emission peaks of the QDs shifted towards lower or higher wavelength, respectively, decreasing the quantum yield. However, no influence from the magnetic environment was reported. Although being built up by means of precipitation of sili-

ca, we have not considered this case to be in the final section because these nanocomposites have both functionalities directly connected in the final form and the silica only serves to hold them together.

There are also very remarkable cases where core and shell dimensions have to be precisely controlled. Different functionalities, in this case magnetic and catalytic (both detailed in a schematic illustration of these nanocomposites, Fig. 6), were also assembled in the same core/shell structured nanoparticles by a redox transmetalation reaction between $Pt(hfac)_2$ (hfac:

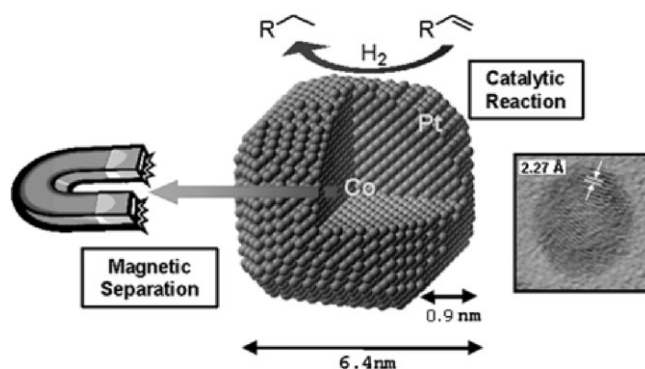


Figure 6. Scheme detailing the magnetic and catalytic functionalities displayed by platinum-coated cobalt nanoparticles. Reproduced with permission from [68]. Copyright 2006 The Royal Society of Chemistry.

hexafluoroacetylacetonate) and previously prepared Co nanocrystals.^[68] After the shell formation, the nanoparticles retained their single-domain superparamagnetism with a blocking temperature of 15 K and a coercivity of 660 Oe ($1 \text{ Oe} = 1000/4\pi \text{ A m}^{-1}$) at 5 K. Core and shell dimensions have to be precisely controlled because it is desirable to minimize the use of Pt as much as possible for economic reasons. However, if the magnetic core is too small, it will not display a strong enough magnetism for magnetic recycling processes. Jun and co-workers designed the synthetic process while taking into account the final applications of the nanoprobes by considering that these platinum coated cobalt nanoparticles should have i) a high surface area for the Pt shell with minimum use of Pt, ii) retention of high magnetism for recycling purposes, and iii) high colloidal stability for the dispersion of the nanocatalysts into the reaction solution.

3.2. Connected Functionalities via Coupling Chemistry

3.2.1. Coupling Chemistry for Organic Dyes

Bifunctionalized core/shell-structured nanoparticles have also been prepared by linking different organic/inorganic components with molecules of different nature, sometimes with the result that the molecule itself patterns the nanoparticle with an additional functionality. Fluorescence labeling by

using small organic dyes has indeed been widely employed in biological systems and for a variety of applications that include diagnostics and biological imaging.^[69] The fabrication of these type of multifunctional nanocomposites ready for biolabeling applications, detectable by both fluorescence and MRI was reported taking into account iron oxide nanoparticles covalently bound to poly(ethylene glycol) (PEG) polymers that were subsequently functionalized with chlorotoxin (a glioma tumor-targeting molecule) and the near-infrared fluorescing (NIRF) molecule Cy5.5.^[70] The use of NIRF molecules allows the visualization of tissues millimeters in depth because of the efficient penetration of photons in the NIR range, as previously mentioned.^[71] On the other hand, PEG coatings help the prevention of nanoparticle agglomeration and protein adsorption, thus increasing particle blood circulation time and the efficiency of their internalization by targeted cells when introduced in vivo. These multifunctional nanocomposites were synthesized by following the procedure outlined in Figure 7. The iron oxide nanoparticles surface was modified with trifluoroethylester-terminated PEG silane, which was then converted to an amine-terminated PEG silane.^[72] Monofunctional *N*-hydroxysuccinimide (NHS) esters of Cy5.5 were then utilized to attach Cy5.5 to the PEG-coated nanoparticles through reaction with the terminal amine groups. Some of these amino groups were also used to conjugate the PEG-coated nanoparticles with chlorotoxin (Cltx). The degree of Cy5.5 labeling of the nanoparticles was controlled through the stoichiometry and reaction conditions, and quantified by fluorescence spectroscopy. The emission intensity of a dilute sample of nanoparticle/Cy5.5 at 689 nm was compared to a linear standard prepared by using various concentrations of Cy5.5. Neither influence of the magnetic material in the fluorescence emission of the conjugated nanocomposites, nor the phenomenon of quenching emission was reported. These iron oxide nanoparticles, conjugated with fluorescence functionality, were targeted to glioma (brain tumor) cells and were detectable both magnetically and optically, thereby proving the potential of these multifunctional systems for the near future.

Bertorelle and co-workers^[73] also reported the synthesis of bifunctional particles that exhibit superparamagnetic and fluorescence properties by coating ferric oxide nanoparticles with fluorescent dyes; rhodamine and fluorescein. The chemi-

cal synthesis was based on the covalent coupling of modified organic fluorophores with *m*-2,3-dimercaptosuccinic acid (DMSA), which strongly interacts with the surface of the ferric oxide nanoparticles. Negative surface charges resulting from the acid–base behavior of grafted DMSA cause repulsive particle interactions and prevent aggregation. In the employed process, the ratio of attached molecules per particle was 10 and 120 for rhodamine B and fluorescein, respectively, which means that the coupling between the fluorescein derivative and the particles is more efficient than the two-stage rhodamine procedure. However, the quantity of the rhodamine B ferrofluid was sufficient in terms of fluorescence, and has the advantage of low cost. The fluorescence intensity of the hybrid nanoparticles was 3.5 times lower than that of fluorescein and two times lower than that of rhodamine because quenching occurs when fluorophores contact a metal surface, and it is possible that the same energy transfer occurs with metal oxide particles. Nevertheless, there is still sufficient emission for biological imaging, and as in the previous case the magnetic properties did not change after the functionalization.

Multistep nanochemistry using a micellar system was suggested for obtaining multifunctional “nanoclinics” for biological applications.^[74] The nanoclinic or nanocomposite consisted of a thin silica shell encapsulating magnetic iron oxide nanoparticles and a fluorescent two-photon dye known as ASPI-SH (1-methyl-4-(*E*)-2-[4-[methyl(2-sulfanylethyl)-amino]phenyl]-1-ethenyl)pyridinium iodide),^[75] which was linked to the iron oxide nanoparticles surface by a thiol group. There was no mention about quenching of the dye fluorescence, which would be expected in the case of directly linkage to the magnetic material. The authors claimed a 20-fold luminescence increased owing to the encapsulation by silica, minimizing the nonradiative decay pathways induced by the surrounding water molecules, which calls our attention to taking into account other cases of silica-coating effects.

3.2.2. Coupling Chemistry for Semiconductor Quantum Dots

QDs are highly luminescent nanoparticles whose absorbance onset and emission maximum shift to higher energy with decreasing particle size, due to quantum confinement effects,^[49] and are brighter, exhibit higher photostability and

show narrower emission peaks compared to organic fluorophores.^[4] The luminescence properties of these semiconductor nanocrystals are very sensitive to their local environment including their surface ligands, rendering therefore their surface functionalization and further coating a key step to be biocompatible.

Iron oxide (γ -Fe₂O₃) nanoparticles (10 nm average diameter) were coated with DMSA to stabilize and functionalize the ferrofluid in aqueous solution.^[76] The surface of the iron oxide

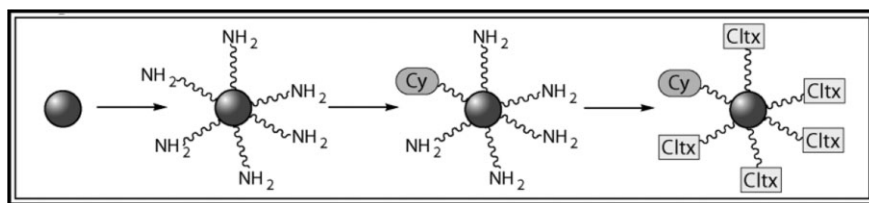


Figure 7. Schematic illustration of the surface of iron oxide nanoparticles modified with PEG molecules, which have been converted to amine-terminated PEG ligands. Monofunctional *N*-hydroxysuccinimide (NHS) esters of Cy5.5 were then utilized to attach Cy5.5 to the PEG-coated nanoparticles through reaction with the terminal amine groups. Some of these amino groups were also used to conjugate the PEG-coated nanoparticles with chlorotoxin (Cltx). Reproduced with permission from [70]. Copyright 2005 The American Chemical Society.

nanoparticles was functionalized with thiols and carboxyl groups to enable further covalent coupling of different ligands to the magnetic nanoparticles. The luminescence functionalization was carried out by means of coupling between luminescent ZnS-coated CdSe QDs and the magnetic beads based on thiol chemistry protocols previously used to stabilize and modify the surface of CdSe QDs.^[77–81] Taking into account that trioctylphosphine oxide (TOPO) molecules stabilize the QDs in chloroform and that magnetic nanoparticles were re-dispersed in aqueous solution, the coupling reaction was carried out in a mixture of chloroform/methanol/water, resulting in minimal aggregation of nanocomposites. These new nanocomposites have an average diameter of 20 nm and display “flower-like” structures, with the QDs imperfectly (with gaps) surrounding the magnetic nanoparticle surface. An example of these nanocomposites is shown in the TEM image of Figure 8. The luminescent properties of the final composites were compared with the initial luminescence from the original ZnS-coated CdSe QDs. A slight blue-shift was observed, and

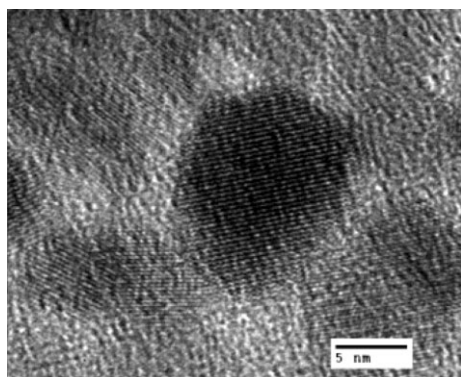


Figure 8. HRTEM image of ZnS-coated CdSe QDs surrounding a magnetic nanoparticle, forming a flower-like structure. Reproduced with permission from [76]. Copyright 2004 The American Chemical Society.

attributed to a change in surface states of the QDs owing to the immobilization process onto the magnetic beads. Furthermore, the quantum yield was found to be around three times lower in the case of the nanocomposites, but the luminescence lifetime was reported to increase. In this case a contribution, and therefore an influence, of the magnetic nanoparticles on the final luminescent properties of the composites was found. These luminescent magnetic nanoparticles were further functionalized with anticycline E molecules by means of carboxylic-group coupling and proved successful in separating and detecting breast cancer cells in serum, underlining the capabilities of this type of material in biological environments.

Various groups have employed a range of wet-chemistry methods to modify or coat the surface of nanoparticles with other colloids. An alternative and already demonstrated promising approach is the layer-by-layer (LbL) self-assembly technique,^[82–85] which offers a versatile route for the creation

of multilayer films of nanoparticulate materials with controllable composition and film thickness; permitting deposition on flat and spherical substrates. By exploiting electrostatic interactions while using the LbL self-assembly technique a range of diverse architectures have been constructed through inserting different functionalities, providing different properties influenced by the particle characteristics (size, shape, and composition), and by the final morphology of the assemblies. Planar solids were first used for the construction of metal-nanoparticle-containing structures,^[86–90] and later spherical colloid particles functioned as supports for the deposition of smaller nanoparticles,^[91–98] designing novel colloids and offering very interesting composite core/shell particles. Thus, the LbL self-assembly technique offers a controllable deposition which has been used for the synthesis of multifunctional materials, in some cases with separated functionalities as will be discussed later.

Magnetic luminescent nanocomposites have been prepared via the LbL assembly approach. Iron oxide nanoparticles of 8.5 nm were used as templates for the deposition of CdTe-QD/polyelectrolyte (PE) multilayers. These multilayered structures, $\text{Fe}_3\text{O}_4/\text{PE}_n/\text{CdTe}$ and $\text{Fe}_3\text{O}_4/(\text{PE}_3/\text{CdTe})_n$, were fabricated following the process outlined in Figure 9.^[99] The large amount of negative charge on the iron oxide surface was favorable for the deposition of charged polyelectrolytes, form-

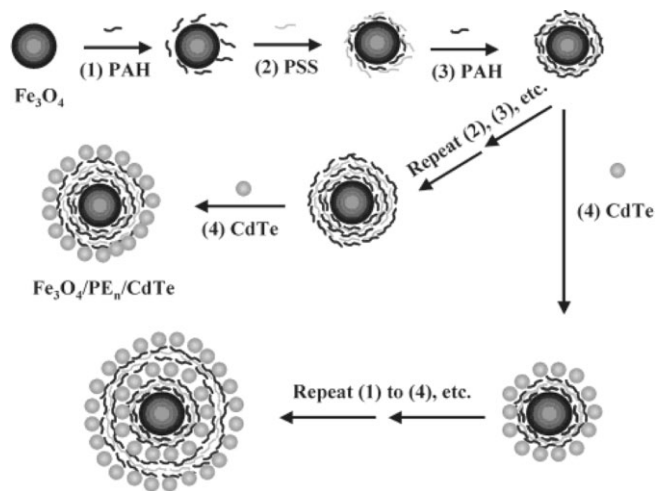


Figure 9. Schematic illustration of the LbL process to form magnetic luminescent $\text{Fe}_3\text{O}_4/\text{CdTe}$ nanocomposites. Reproduced with permission from [99]. Copyright 2004 The American Chemical Society.

ing uniform multilayers. Thereby, the thickness of the polyelectrolyte interlayer film can be controlled and therefore the distance between the magnetic and the luminescent nanoparticles in the final nanocomposites can be tuned. The photoluminescence (PL) intensity was demonstrated to be very sensitive to the distance between the iron oxide nanoparticles and the CdTe QDs, and was enhanced with increasing thickness of the polyelectrolyte interlayers, reaching a plateau after 21

polyelectrolyte layers. Taking into account that the polyelectrolyte multilayers themselves do not change the PL signal from the CdTe QDs,^[100] this influence can only be caused by an interaction between the Fe₃O₄ and the QDs that leads to energy transfer.^[101] On the other hand, the surface area of a single particle increases with an increased number of adsorbed polyelectrolyte layers, permitting much more CdTe QDs to be deposited on the surface of every iron oxide nanoparticle; however, this increase was confined to a certain region. The influence on the PL was considered by Hong and co-workers^[99] to be a cooperative effect of the two factors, the distance and the concentration. As a second option, Fe₃O₄/(PE₃/CdTe)_n were also prepared by repetitious deposition of (PE₃/CdTe)_n onto the iron oxide nanoparticles, observing a linear increase of the CdTe QDs absorbance versus the corresponding deposition number which indicated a stepwise and uniform assembling process.

3.2.3. Coupling Chemistry for Metallic Nanoparticles

The bottom-up LbL self-assembly approach has also been used to deposit magnetic and optically active nanoparticles onto spherical substrates, since it allows to independently control the magnetic moment and the optical properties. By choosing a number of biocompatible magnetite layers, the magnetic moment per sphere can be tuned while simultaneously the number of adsorbed gold nanoparticle layers determines the optical response.^[102] These composite core/shell particles combine the magnetic and optical properties of the individual magnetite and silica-coated gold nanoparticles (Fig. 10). The magnetic properties allow a magnetic field re-directioning, that is, magnetophoretic self-assembly into ordered structures, while their optical properties, monitored through UV-vis spectrometry, were found to be similar to systems without magnetite. There is no influence of the magnetic material on the surface plasmon band of the closely deposited gold nanoparticles because of the silica shell spacer and the polyelectrolyte layers in between the two types of functionalities. The absence of the silica shell spacer in a very similar system of gold nanoparticles deposited onto planar substrates together with magnetite implied an influence on the surface plasmon band.^[103]

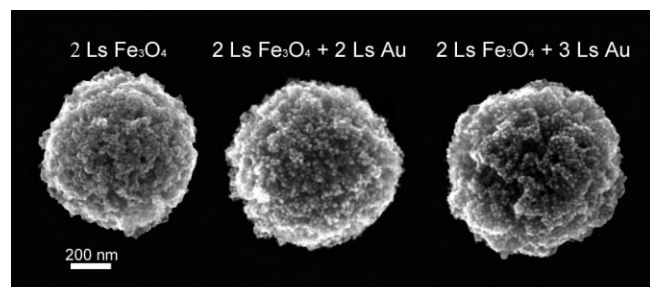


Figure 10. SEM images of polystyrene spheres coated with a different number of layers of magnetite and silica-coated gold nanoparticles. Reproduced with permission from [102]. Copyright 2005 The Royal Society of Chemistry.

3.3. Silica-Based Isolated Functionalities

In a more generic approach, different building blocks can be assembled into active nanocomposites (prepared following designed strategies that include successive combination of processes) in such a way that the inserted functionalities are kept separated in the final structure. This can be accomplished by using silica which permits the assembly of different materials carrying one, two, or several functionalities, sometimes by using the covalent bonding of organic molecules. This covalent bonding through grafting procedures for silica using commercially available silane coupling agents is well-established^[104,105] with different functional groups to be attached or incorporated, taking advantage of the hydroxy (Si–OH) and ethoxy (Si–OCH₂CH₃) groups that predominate before modification.^[106] These groups can be treated with different terminated trialkoxyorganosilanes to modify the silica in such a manner that CH₃, PPh₂, NH₂ or SH functional groups will be available,^[107] and depending on the final achievement involving silica a different functionality can be included.

The sol–gel method based on the hydrolysis of tetraethyl orthosilicate (TEOS) was used by Lu and co-workers for coating iron oxide nanoparticles with uniform shells, where fluorescent dyes were incorporated through covalent coupling.^[108] The covalent bond formed in this reaction can stabilize the fluorescent dye and simultaneously can chemically incorporate it into the silica shell by co-hydrolyzing the APS with TEOS. A very similar approach was recently developed to coat superparamagnetic iron oxide nanoparticles with silica, hydrolyzing TEOS, and *N*-1-(3-trimethoxysilylpropyl)-*N'*-fluoresceylthiourea, producing fluorescent magnetic nanoparticles for the development of contrast agents with which stem cells could be efficiently and harmlessly labeled and subsequently imaged with a clinical MRI analyzer at low cell numbers.^[109]

This base-catalyzed hydrolysis of TEOS to precipitate silica has also been used on iron oxide nanoparticles (average diameter 10 nm) together with the LbL self-assembly technique, driving CdTe QDs (average diameter 3 nm) or Au nanoparticles (average diameter 15 nm) onto the surface of the magnetic particles previously coated with silica. Salgueiriño-Maceira and co-workers were able to combine these two processes to yield luminescent and magnetic or gold-coated silica spheres,^[110,111] without interaction between the optical and magnetic functionalities, as these were efficiently separated by a thick silica shell. The silica-coated iron oxide particles used for the production of these bifunctional core/shell composites have a core diameter of about 30 nm and a silica shell thickness of 70 nm, yielding an average total diameter of (170 ± 10) nm, ensuring no influence from the magnetic core onto the external optically active materials. These magnetic silica spheres were shown to be superparamagnetic, with a saturation magnetization of 1.34 emu g^{−1} at 300 K, allowing the nanoparticles to be easily magnetized for efficient magnetic separation in an external magnetic field. In order to impart the second optical functionality to these magnetic silica

spheres, CdTe QDs^[112] and Au nanoparticles^[113] were synthesized and self-assembled onto their surfaces following the schemes illustrated in Figure 11. Both CdTe QDs and Au nanocrystals were deposited onto the surface of silica-coated iron oxide particles by using the LbL self-assembly method explained above. The PL of the original QD dispersion and the surface plasmon band of the gold nanoparticles were retained in the final composites. The normalized PL emission spectrum of QDs deposited onto the magnetic composite particles was blue-shifted (around 5 nm) compared to the free QDs in water, behavior that has been already reported for CdSe QDs.^[114,115] In this case, the thiol ligands that stabilized the QDs in solution may have been converted to disulfides under light irradiation and during the LbL process, yielding unprotected CdTe QDs on the surface of the magnetic silica spheres, which would explain the spectral shift toward shorter wavelengths, but keeping the feature of no influence between the different functionalities in the final composite. To increase the colloidal and chemical stability, the composite magnetic luminescent spheres were additionally coated with an outer layer of silica (nm average thickness 20),^[116] as indicated in the top scheme of Figure 11. To elucidate how the silica coating affects the photoluminescence, spectra of the composite particles were measured before and after the deposition of the outer silica shell, again observing a blue-shift of the emission spectra (10 nm). Although previous reports showed different results concerning the effect of the silica coating on the luminescent properties of QDs, in this case of CdTe nanocrystals, they may continuously undergo corrosion during the silica deposition because thiol ligands must be totally removed from their surface, leaving the QDs unprotected and resulting in the observed blue-shift in the maximum of the emission spectra. Even if the outer silica shell can not totally prevent corrosion of the CdTe QDs, it does improve the chemical and colloidal stability of the luminescent magnetic nanocomposites and offers an ideal anchorage substrate for the covalent binding of specific ligands. In the second approach, 15 nm gold colloids were attached onto the surface of magnetic silica spheres to initiate the growth of a solid gold shell (bottom scheme in Fig. 12).^[117,118] This formation of the solid outer shell can be monitored by UV-vis spectroscopy, following the red-shift of the surface plasmon band while completing the gold shell. Once the shell is complete (30 nm thick, as determined by TEM) the peak absorbance reaches the NIR range, in close agreement with theoretical calculations.^[119,120] Both types of bifunctional particles (luminescent and gold-coated magnetic silica spheres) can be directed to specific locations when manipulated by an external magnetic field,

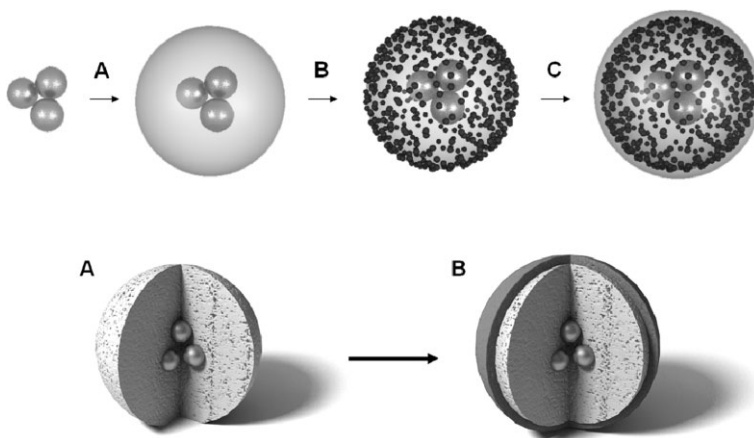


Figure 11. Schemes of the different steps followed to prepare magnetic and luminescent nanocomposites (top) and gold-coated magnetic silica spheres (bottom). Reproduced with permission from [110]. Copyright 2006 The American Chemical Society.

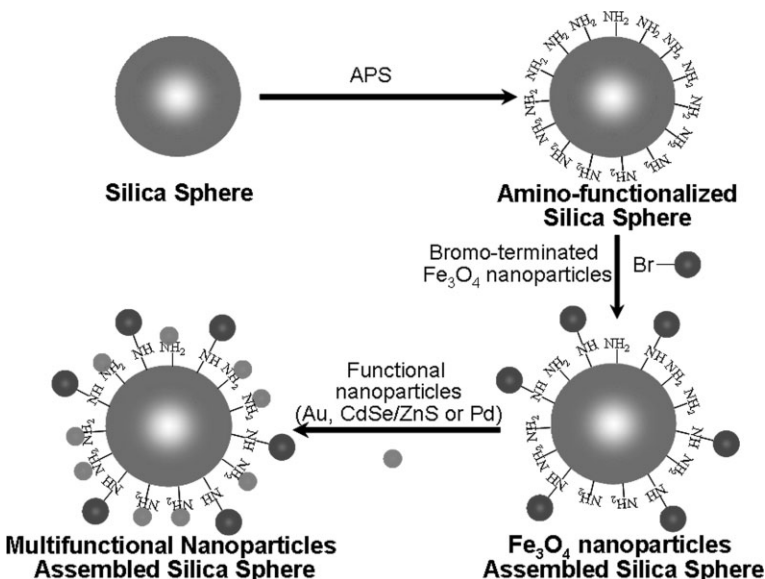


Figure 12. Diagram of the functionalization of the silica spheres surface with APS and adsorption of magnetite nanoparticles. Taking into account the remaining NH₂ groups; Au, CdSe/Zn and/or Pd nanoparticles were further adsorbed giving place to multifunctionalized silica spheres. Reproduced from [121].

which furthermore can be easily monitored through the intense optical properties they display.

Multifunctionality has also been imparted to nanometer-sized particles by means of a nucleophilic substitution reaction in organic media (indicated in the scheme of Fig. 12),^[121] which should be considered as an assembly of functionalities via coupling chemistry. However, in this case the coupling chemistry was used to bind the building blocks to silica spheres instead of coupling the different functionalities themselves, thereby considering them as isolated functionalities with no influence reported. Amino-functionalized silica spheres were used as substrates on which to bring together

nanoparticles of Fe_3O_4 , Au, CdSe/ZnS, or Pd, giving place to multifunctional silica spheres that exhibited a combination of magnetism and surface plasmon resonance, luminescence, or catalysis. The key step in this case was the previous functionalization of the surface of the silica spheres with amino groups by treatment with APS and the fact that the capping agents of the magnetic nanoparticles to be deposited onto the silica spheres surface were exchanged with 2-bromo-2-methylpropionic acid (BMPA).^[122] The BMPA-stabilized nanoparticles were therefore covalently bonded onto the surfaces of the amino-functionalized silica spheres by a direct nucleophilic substitution reaction between the terminal Br atoms of the ligands and the NH_2 groups on the silica spheres in THF.^[123] Subsequently, taking into account that the number of magnetic nanoparticles deposited onto the functionalized silica spheres is much lower than the number of available amino groups, the remaining amino groups were used for a further deposition of nanoparticles of a different nature, permitting the multifunctionality by attaching not only magnetic, but also metallic nanoparticles and semiconductor QDs.

A second case, which could also match with a different section of this Review, was chosen to be labeled as composites with isolated but interacting functionalities because of the reasons below. The LbL self-assembly technique can also be combined with electron beam evaporation (EBE) as a different approach to obtain asymmetrically functionalized bimetallic silica spheres.^[43] As a first step, silica-coated gold nanoparticles (core diameter 18 nm and shell thickness 8 nm) were deposited onto the surface of larger silica spheres following the LbL self-assembly technique, in a manner similar to the previously published cases of silica-coated gold nanoparticles on polystyrene spheres.^[97,98] This step led to the formation of a very homogeneous layer of silica-coated gold nanoparticles on the surface of silica spheres used as substrates. Upon coating, the resulting composite colloids were covered with a half-shell of nickel by EBE, giving place to magnetic half-shells on the surface of the already coated silica spheres. Figure 13a and b shows a schematic illustration of these asymmetrically functionalized silica spheres and an SEM image, respectively, showing the different roughness, contrast, and thickness of the two sides of the spheres depending on the silica-coated gold nanoparticles deposited onto one of the hemispheres (right side of the particle) or the evaporated metallic nickel onto the silica-coated gold nanoparticles on the second hemisphere (left side of the particle).

The optical properties of these asymmetrically functionalized silica spheres are reminiscent of the surface plasmon resonance of the deposited individual gold nanoparticles. In this case, likely owing to a large increase in the dielectric constant of the surroundings of the monolayer of silica-coated gold nanoparticles upon nickel deposition, the plasmon band redshifts up to 770 nm. In addition, the presence of Ni half-shells also provides these asymmetrically bifunctionalized nanocomposites with magnetic properties, and under a homogeneous in-plane magnetic field these colloids can indeed be aligned

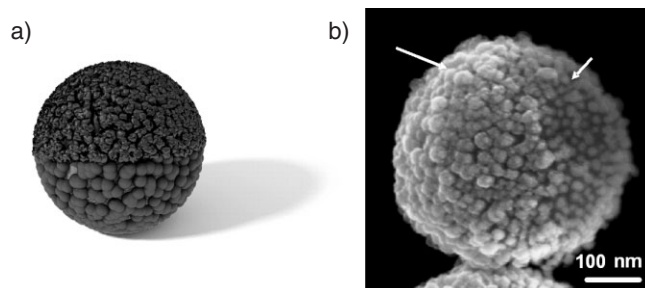


Figure 13. Illustration (a) and SEM image (b) of an asymmetrically coated silica sphere, coated with a monolayer of silica-coated gold nanoparticles and an outer half-shell of nickel. Reproduced from [43].

along the direction of the applied field. The silica shell surrounding the gold nanoparticles maintains both functionalities separated although still interacting, permitting us to classify these composites as silica-based nanocomposites with isolated functionalities.

4. Conclusion and Outlook

This is a brief overview of the many efforts that have been employed in the development of new multifunctional nanocomposites, which present promising applications in several fields, although generally related with the biological environment. Nanocomposite systems are increasing in complexity in terms of both structure and functionalities (interacting or not), given this complexity by new methods of synthesis that are generating the most rapid advances. Coupling chemistry, silica precipitation, and metals salts reduction are now routinely used within a very wide range of processes to yield these versatile nanocomposites of almost any desired structure. Silica is an example of a key component of these nanometer-scale materials that, combined with coupling chemistry and molecular biology, is enabling these highlighted structures to extend across the biomedical field.

The synthesis reports included in this Review demonstrate the high control in the final structure at the nanometer scale, using different functional material as building blocks to be assembled and tuning the interactions between already existing functionalities to further increase the range of possibilities in future applications. We have restricted the range of multifunctional structures to the core/shell morphology, but as in this case, other examples including the dimers pointed out in this report, are increasing exponentially, answering key questions in many different fields, continually emerging in different applications although with still much more to explore. Future research is being directed to improving the demanded individual and collective properties of the multifunctional nanocomposites, developing new features, and easy and reproducible methods that should permit low-cost production on a practical scale. Multifunctional nanocomposites can be envisioned as a

new generation of materials with advantageous properties for the improvement and development of new, useful, and commercially viable applications.

Received: February 15, 2007

Revised: May 30, 2007

Published online: October 31, 2007

- [1] D. P. O'Neal, L. R. Hirsch, N. J. Halas, J. D. Payne, J. L. West, *Cancer Lett.* **2004**, 209, 171.
- [2] X. Gao, Y. Cui, R. M. Levenson, L. W. K. Chung, S. Nie, *Nat. Biotechnol.* **2004**, 22, 969.
- [3] J. L. West, N. J. Halas, *Curr. Opin. Biotechnol.* **2000**, 11, 215.
- [4] W. C. W. Chan, S. Nie, *Science* **1998**, 281, 2016.
- [5] X. Michalet, F. F. Pinaud, L. A. Bentolila, J. M. Tsay, S. Doose, J. J. Li, G. Sundaresan, A. M. Wu, S. S. Gambhir, S. Weiss, *Science* **2005**, 307, 538.
- [6] O. Rabin, J. M. Perez, J. Grimm, G. Wojtkiewicz, R. Weissleder, *Nat. Mater.* **2006**, 5, 118.
- [7] M. Ferrari, *Nat. Rev. Cancer* **2005**, 5, 161.
- [8] G. M. Whitesides, *Nat. Biotechnol.* **2003**, 21, 1161.
- [9] I. L. Medintz, H. T. Uyeda, E. R. Goldman, H. Mattoussi, *Nat. Mater.* **2005**, 4, 435.
- [10] B. Dubertret, P. Skourides, D. J. Norris, V. Noireaux, A. H. Brivanlou, A. Libchaber, *Science* **2002**, 298, 1759.
- [11] S. Kim, Y. T. Lim, E. G. Soltesz, A. M. De Grand, J. Lee, A. Nakayama, J. A. Parker, T. Mihaljevic, R. G. Laurence, D. M. Dor, L. H. Cohn, M. G. Bawendi, J. V. Frangioni, *Nat. Biotechnol.* **2004**, 22, 93.
- [12] P. Tartaj, M. P. Morales, S. Veintemillas-Verdaguer, T. González-Carreño, C. J. Serna, *J. Phys. D* **2003**, 36, R182.
- [13] Q. A. Pankhurst, J. Connolly, S. K. Jones, J. Dobson, *J. Phys. D* **2003**, 36, R167.
- [14] T. Shen, R. Weissleder, M. Papisov, A. Bogdanov, Jr., T. J. Brady, *Magn. Reson. Med.* **1993**, 29, 599.
- [15] S. Santra, H. Yang, P. H. Holloway, J. T. Stanley, R. A. Mericle, *J. Am. Chem. Soc.* **2005**, 127, 1656.
- [16] I. H. El-Sayed, X. Huang, M. A. El-Sayed, *Nano Lett.* **2005**, 5, 829.
- [17] J. Chen, F. Saeki, B. J. Wiley, H. Cang, M. J. Cobb, Z. Y. Li, L. Au, H. Zhang, M. B. Kimmey, X. Li, Y. Xia, *Nano Lett.* **2005**, 5, 473.
- [18] J. F. Hulvat, S. I. Stupp, *Adv. Mater.* **2004**, 16, 589.
- [19] T. Teranishi, Y. Inoue, M. Nakaya, Y. Oumi, T. Sano, *J. Am. Chem. Soc.* **2004**, 126, 9914.
- [20] K.-H. Roh, D. C. Martin, J. Lahann, *Nat. Mater.* **2005**, 4, 759.
- [21] D. L. Leslie-Pelecky, R. D. Rieke, *Chem. Mater.* **1996**, 8, 1770.
- [22] D. Jiles, *Introduction to Magnetism and Magnetic Materials*, Chapman and Hall, London **1991**.
- [23] A. H. Morrish, *The Physical Principles of Magnetism*, IEEE, New York **2001**.
- [24] W. Heukelom, J. J. Broeder, L. L. Van Reijen, *J. Chim. Phys. Phys.-Chim. Biol.* **1954**, 51, 474.
- [25] L. Néel, *C. R. Acad. Sci.* **1949**, 228, 664.
- [26] C. P. Bean, J. D. Livingston, *J. Appl. Phys.* **1959**, 30, 120S.
- [27] C. P. Bean, I. S. Jacobs, *J. Appl. Phys.* **1956**, 27, 1448.
- [28] E. C. Stoner, E. P. Wohlfarth, *Proc. Phys. Soc. A* **1948**, 240, 599.
- [29] K. O'Grady, *J. Phys. D* **2003**, 36.
- [30] N. Nasongkla, E. Bey, J. Ren, H. Ai, C. Khemtong, J. S. Guthi, S.-F. Chin, A. D. Sherry, D. A. Boothman, J. Gao, *Nano Lett.* **2006**, 6, 2427.
- [31] U. Kreibitz, M. Vollmer, *Optical Properties of Metal Clusters*, Springer, Berlin **1996**.
- [32] P. Mulvaney, *Langmuir* **1996**, 12, 788.
- [33] S. J. Oldenburg, J. B. Jackson, S. L. Westcott, N. J. Halas, *Appl. Phys. Lett.* **1999**, 75, 2897.
- [34] R. Weissleder, *Nat. Biotechnol.* **2001**, 19, 316.
- [35] K. R. Brown, D. G. Walter, M. J. Natan, *Chem. Mater.* **2000**, 12, 306.
- [36] J. L. Lyon, D. A. Fleming, M. B. Stone, P. Schiffer, M. E. Williams, *Nano Lett.* **2004**, 4, 719.
- [37] J. Jeong, T. H. Ha, B. H. Chung, *Anal. Chim. Acta* **2006**, 569, 203.
- [38] S. J. Oldenburg, R. D. Averitt, S. L. Westcott, N. J. Halas, *Chem. Phys. Lett.* **1998**, 288, 243.
- [39] J. Lin, W. Zhou, A. Kumbhar, J. Wiemann, J. Fang, E. E. Carpenter, C. J. O'Connor, *J. Solid State Chem.* **2001**, 159, 26.
- [40] G. K. Kouassi, J. Irudayaraj, *Anal. Chem.* **2006**, 78, 3234.
- [41] H. Yu, M. Chen, P. M. Rice, S. X. Wang, R. L. White, S. Sun, *Nano Lett.* **2005**, 5, 379.
- [42] M.-C. Daniel, D. Astruc, *Chem. Rev.* **2004**, 104, 293.
- [43] M. A. Correa-Duarte, V. Salgueiriño-Maceira, B. Rodríguez-González, L. M. Liz-Marzán, A. Kosiorek, W. Kandulski, M. Giersig, *Adv. Mater.* **2005**, 17, 2014.
- [44] W. Stöber, A. Fink, E. Bohn, *J. Colloid Interface Sci.* **1968**, 26, 62.
- [45] Z. Nie, W. Li, M. Seo, S. Xu, E. Kumacheva, *J. Am. Chem. Soc.* **2006**, 128, 9408.
- [46] T. Nisisako, T. Torii, T. Takahashi, Y. Takizawa, *Adv. Mater.* **2006**, 18, 1152.
- [47] B. Valeur, *Molecular Fluorescence*, Wiley-VCH, Weinheim, Germany **2002**.
- [48] M. Bruchez, Jr., M. Moronne, P. Gin, S. Weiss, A. P. Alivisatos, *Science* **1998**, 281, 2013.
- [49] A. Waggoner, *Methods Enzymol.* **1995**, 246, 362.
- [50] P. Alivisatos, *J. Phys. Chem.* **1996**, 100, 13 226.
- [51] R. Bratschitsch, A. Leitenstorfer, *Nat. Mater.* **2006**, 5, 855.
- [52] P. Alivisatos, *Nat. Biotechnol.* **2004**, 22, 47.
- [53] F. Tokumasu, J. Dvorak, *J. Microsc.* **2003**, 211, 256.
- [54] D. S. Lidke, P. Nagy, R. Heintzmann, D. J. Arndt-Jovin, J. N. Post, H. E. Grecco, E. A. Jares-Erijman, T. M. Jovin, *Nat. Biotechnol.* **2004**, 22, 198.
- [55] S. Pathak, S. K. Choi, N. Arnheim, M. E. Thompson, *J. Am. Chem. Soc.* **2001**, 123, 4103.
- [56] X. Michalet, F. Pinaud, A. Weiss, *Single Mol.* **2001**, 2, 261.
- [57] H. Kim, M. Achermann, L. P. Balet, J. A. Hollingsworth, V. I. Klimov, *J. Am. Chem. Soc.* **2005**, 127, 544.
- [58] Y. Labaye, O. Crisan, L. Berger, J. M. Greneche, J. M. D. Coey, *J. Appl. Phys.* **2002**, 91, 8715.
- [59] G. C. Papaefthymiou, *Mater. Res. Soc. Symp. Proc.* **2001**, 635, C241.
- [60] X.-Y. Wang, J.-Y. Zhang, A. Nazzal, M. Darragh, M. Xiao, *Appl. Phys. Lett.* **2002**, 81, 4829.
- [61] A. L. Efros, M. Rosen, M. Kuno, M. Nirmal, D. J. Norris, M. Bawendi, *Phys. Rev. B* **1996**, 54, 4843.
- [62] H. Gu, R. Zheng, X. Zhang, B. Xu, *J. Am. Chem. Soc.* **2004**, 126, 5664.
- [63] H. Lu, G. Yi, S. Zhao, D. Chen, L.-H. Guo, J. Cheng, *J. Mater. Chem.* **2004**, 14, 1336.
- [64] H.-Y. Xie, C. Zuo, Y. Liu, Z.-L. Zhang, D.-W. Pang, X.-L. Li, J.-P. Gong, C. Dickinson, W. Zhou, *Small* **2005**, 1, 506.
- [65] X. Zhao, Y. Liu, H. Hui, *J. Med. Coll. PLA* **1997**, 12, 62.
- [66] G.-P. Wang, E.-Q. Song, H.-Y. Xie, Z.-L. Zhang, Z.-Q. Tian, C. Zuo, D.-W. Pang, D.-C. Wu, Y.-B. Shi, *Chem. Commun.* **2005**, 4276.
- [67] D. K. Yi, S. T. Selvan, S. S. Lee, G. C. Papaefthymiou, D. Kundaliya, J. Y. Ying, *J. Am. Chem. Soc.* **2005**, 127, 4990.
- [68] C.-H. Jun, Y.-J. Park, Y.-R. Yeon, J.-r. Choi, W.-r. Lee, S.-j. Ko, J. Cheon, *Chem. Commun.* **2006**, 1619.
- [69] E. Schröck, S. du Manoir, T. Veldman, B. Schoell, J. Wienberg, M. A. Ferguson-Smith, Y. Ning, D. H. Ledbetter, I. Bar-Am, D. Soenksen, Y. Garini, T. Ried, *Science* **1996**, 273, 494.
- [70] O. Vieseh, C. Sun, J. Gunn, N. Kohler, P. Gabikian, D. Lee, N. Bhattarai, R. Ellenbogen, R. Sze, A. Hallahan, J. Olson, M. Zhang, *Nano Lett.* **2005**, 5, 1003.
- [71] R. Weissleder, V. Ntziachristos, *Nat. Med.* **2003**, 9, 123.
- [72] N. Kohler, G. E. Fryxell, M. Q. Zhang, *J. Am. Chem. Soc.* **2004**, 126, 7206.

- [73] F. Bertorelle, C. Wilhelm, J. Roger, F. Gazeau, C. Ménager, V. Caubuil, *Langmuir* **2006**, 22, 5385.
- [74] L. Levy, Y. Sahoo, K.-S. Kim, E. J. Bergey, P. N. Prasad, *Chem. Mater.* **2002**, 14, 3715.
- [75] M. Lal, L. Levy, K. S. Kim, G. S. He, X. Wang, Y. H. Min, S. Pakatchi, P. N. Prasad, *Chem. Mater.* **2000**, 12, 2632.
- [76] D. Wang, J. He, N. Rosenzweig, Z. Rosenzweig, *Nano Lett.* **2004**, 4, 409.
- [77] D. Gerion, F. Pinaud, S. C. William, W. J. Parak, D. Zanchet, S. Weiss, A. P. Alivisatos, *J. Phys. Chem. B* **2001**, 105, 8861.
- [78] Y. A. Wang, J. J. Li, H. Chen, X. Peng, *J. Am. Chem. Soc.* **2002**, 124, 2293.
- [79] C. Zhang, S. O'Brien, L. Balogh, *J. Phys. Chem. B* **2002**, 106, 10316.
- [80] S. F. Wuister, I. Swart, F. V. Driel, S. G. Hickey, C. M. Donega, *Nano Lett.* **2003**, 3, 503.
- [81] J. Aldana, Y. A. Wang, X. Peng, *J. Am. Chem. Soc.* **2001**, 123, 8844.
- [82] G. Decher, J. D. Hong, *Ber. Bunsen-Ges.* **1991**, 95, 1430.
- [83] N. A. Kotov, I. Dekany, J. H. Fendler, *J. Phys. Chem.* **1995**, 99, 13065.
- [84] G. Decher, *Science* **1997**, 277, 1232.
- [85] F. Caruso, *Adv. Mater.* **2001**, 13, 11.
- [86] D. I. Gittins, D. Bethell, R. J. Nichols, D. J. Schiffrin, *Adv. Mater.* **1999**, 11, 737.
- [87] J. Schmitt, G. Decher, W. J. Dressick, S. L. Brandow, R. E. Geer, R. Shashidhar, J. M. Calvert, *Adv. Mater.* **1997**, 9, 61.
- [88] D. L. Feldheim, K. C. Grabar, M. J. Natan, T. E. Mallouk, *J. Am. Chem. Soc.* **1996**, 118, 7640.
- [89] T. Cassagneau, J. H. Fendler, *J. Phys. Chem. B* **1999**, 103, 1789.
- [90] M. Alejandro-Arellano, T. Ung, A. Blanco, P. Mulvaney, L. M. Liz-Marzán, *Pure Appl. Chem.* **2000**, 72, 257.
- [91] F. Caruso, H. Lichtenfeld, M. Giersig, H. Möhwald, *J. Am. Chem. Soc.* **1998**, 120, 8523.
- [92] F. Caruso, H. Möhwald, *Langmuir* **1999**, 15, 8276.
- [93] F. Caruso, A. S. Sussha, M. Giersig, H. Möhwald, *Adv. Mater.* **1999**, 11, 950.
- [94] F. Caruso, M. Spasova, A. Sussha, M. Giersig, R. A. Caruso, *Chem. Mater.* **2001**, 13, 109.
- [95] R. A. Caruso, A. Sussha, F. Caruso, *Chem. Mater.* **2001**, 13, 400.
- [96] K. H. Rhodes, S. A. Davis, F. Caruso, B. Zhang, S. Mann, *Chem. Mater.* **2000**, 12, 2832.
- [97] F. Caruso, M. Spasova, V. Salgueiriño-Maceira, L. M. Liz-Marzán, *Adv. Mater.* **2001**, 13, 1090.
- [98] V. Salgueiriño-Maceira, F. Caruso, L. M. Liz-Marzán, *J. Phys. Chem. B* **2003**, 107, 10990.
- [99] X. Hong, J. Li, M. Wang, J. Xu, W. Guo, J. Li, Y. Bai, T. Li, *Chem. Mater.* **2004**, 16, 4022.
- [100] O. Kulakovich, N. Strekal, A. Yaroshevich, S. Maskevich, S. Gaponenko, I. Nabiev, U. Woggon, M. Artemyev, *Nano Lett.* **2002**, 2, 1449.
- [101] V. F. Agekyan, *Phys. Solid State* **2002**, 44, 2013.
- [102] M. Spasova, V. Salgueiriño-Maceira, A. Schlachter, M. Hilgendorff, M. Giersig, L. M. Liz-Marzán, M. Farle, *J. Mater. Chem.* **2005**, 15, 2095.
- [103] V. Salgueiriño-Maceira, M. A. Correa-Duarte, M. A. López-Quintela, J. Rivas, *Sens. Lett.* **2007**, 5, 113.
- [104] A. P. Philipse, A. Vrij, *J. Colloid Interface Sci.* **1989**, 128, 121.
- [105] A. van Blaaderen, A. Vrij, *Langmuir* **1992**, 8, 2921.
- [106] R. D. Badley, W. T. Ford, F. J. McEnroe, R. A. Assink, *Langmuir* **1990**, 6, 792.
- [107] S. L. Wescott, S. J. Oldenburg, T. Randall Lee, N. J. Halas, *Langmuir* **1998**, 14, 5396.
- [108] Y. Lu, Y. Yin, B. T. Mayers, Y. Xia, *Nano Lett.* **2002**, 2, 183.
- [109] C.-W. Lu, Y. Hung, J.-K. Hsiao, M. Yao, T.-H. Chung, Y.-S. Lin, S.-H. Wu, S.-C. Hsu, H.-M. Liu, C.-Y. Mou, C.-S. Yang, D.-M. Huang, Y.-C. Chen, *Nano Lett.* **2007**, 7, 149.
- [110] V. Salgueiriño-Maceira, M. A. Correa-Duarte, M. Farle, M. A. López-Quintela, K. Sieradzki, R. Díaz, *Chem. Mater.* **2006**, 18, 2701.
- [111] V. Salgueiriño-Maceira, M. A. Correa-Duarte, M. Spasova, L. M. Liz-Marzán, M. Farle, *Adv. Funct. Mater.* **2006**, 16, 509.
- [112] N. Gaponik, D. V. Talapin, A. L. Rogach, K. Hoppe, E. V. Shevchenko, A. Kornowski, A. Eychmüller, H. Weller, *J. Phys. Chem. B* **2002**, 106, 7177.
- [113] V. Enustün, J. Turkevich, *J. Am. Chem. Soc.* **1963**, 85, 3317.
- [114] Y. Wang, Z. Tang, M. A. Correa-Duarte, I. Pastoriza-Santos, M. Giersig, N. A. Kotov, L. M. Liz-Marzán, *J. Phys. Chem. B* **2004**, 108, 15461.
- [115] M. Nirmal, B. O. DAbbousi, M. G. Bawendi, J. J. Macklin, J. K. Trautman, T. D. Harris, L. E. Brus, *Nature* **1996**, 383, 802.
- [116] V. Salgueiriño-Maceira, M. Spasova, M. Farle, *Adv. Funct. Mater.* **2005**, 15, 1036.
- [117] S. J. Oldenburg, S. L. Westcott, R. D. Averitt, N. J. Halas, *J. Chem. Phys.* **1999**, 111, 4729.
- [118] C. Graf, A. van Blaaderen, *Langmuir* **2002**, 18, 524.
- [119] C. Radloff, N. J. Halas, *Nano Lett.* **2004**, 4, 1323.
- [120] E. Prodan, C. Radloff, N. J. Halas, P. Nordlander, *Science* **2003**, 302, 419.
- [121] J. Kim, J. E. Lee, J. Lee, Y. Jang, S.-W. Kim, K. An, J. H. Yu, T. Hyeon, *Angew. Chem. Int. Ed.* **2006**, 45, 4789.
- [122] Y. Wang, X. Teng, J.-S. Wang, H. Yang, *Nano Lett.* **2003**, 3, 789.
- [123] S.-S. Bae, D. K. Lim, J.-I. Park, W.-R. Lee, J. Cheon, S. Kim, *J. Phys. Chem. B* **2004**, 108, 2575.